Specific Solute−Solvent Interactions: The Ethene$^+$...Ar Complex

Gregory D. Scholes,*,† Richard D. Harcourt,‡ Ian R. Gould,† and David Phillips†

Department of Chemistry, Imperial College of Science, Technology and Medicine, Exhibition Road, London SW7 2AY, United Kingdom, and School of Chemistry, The University of Melbourne, Parkville, Victoria 3052, Australia

Received: July 8, 1996; In Final Form: October 30, 1996[⊗]

A molecule-based description of charge delocalization is introduced to describe interactions which depend upon intermolecular orbital overlap in order to investigate the origin of stabilization in specific solute−solvent complexes. Ionization potentials of aromatic "solute" molecules are shifted to lower energy in rare gas clusters, which has been attributed previously to charge−induced dipole interactions; however, the present work reveals that a charge "delocalization" mechanism may be operative in certain systems. This is due primarily to charge-transfer (CT) effects. A relationship between this interaction and the difference between solute and solvent ionization potentials is derived. The ethene$^+$...Ar complex is examined as a specific case. We report the results of *ab initio* molecular orbital (MO), localized molecular orbital (LMO), and valence-bond (VB) studies of the $C_2H_4^+$...Ar complex to provide a VB rationalization for the origin of the stability of the complex. The advantage of the VB treatment employed in the present work is that it allows a natural separation between polarization and CT terms, so it could be shown that the CT interaction provides a key contribution to the stabilization of the $C_2H_4^+$...Ar complex. These results suggest that intermolecular charge-transfer resonances may to play a significant role in delocalizing charge among a charged ("solute") molecule and suitably proximate neutral ("solvent") molecules in a cluster.

1. Introduction

Charge stabilization by solvent is a fundamental component of a variety of photophysical processes in the condensed phase and clusters. It is well-known that charged species are stabilized in a dielectric continuum with respect to a vacuum. Accordingly, it is usual to approximate the effect of solvent outside the saturated solvent shells (for example, in electron-transfer reactions) as a dielectric continuum.[1−3] Such a theoretical formulation is best used with the caveat that it is not suitable for cases where a charge-transfer complex is strongly bound, or where there is some specific interaction with surrounding molecules.[4] Molecular aspects of the solute−solvent interaction have been examined experimentally recently.[5] In the present work we focus upon solvation of a charged molecule or atom in a cluster.

The present work was motivated by the question: "Can we ignore the molecular identity of the inner sphere solvent?" In other words, what is the role of *specific* solvent effects? Such a query is not new, but has inspired a number of experimental and theoretical studies of the microscopic solvation in ion−solvent clusters which explore the transition from complexes to bulk system.[6−8] The interplay between the usual long-range interactions and specific short-range interactions is of interest in such systems. In the present work we introduce a *microscopic* (i.e., molecule-based) quantum chemical description of the interactions within a charged "solute"/neutral "solvent" cluster. We examine the role and significance of interactions which depend upon solute−solvent orbital overlap. We highlight some relevant experimental examples and investigate the ethene$^+$...Ar complex as a specific case.

Even in the bulk condensed phase, the formation of specific solute−solvent complexes of the type described in the present work may have significant implications. It has been proposed that, for the anomalous, TICT (twisted intramolecular charge transfer) state, emission from 4-(dimethylamino)benzonitrile (DMABN) may originate primarily from specific solute−solvent complexes (solute−solvent exciplexes).[9] Quite a number of studies of DMABN in a free jet expansion have attempted to elucidate this issue.[10] A further example of interest is that of electron-donating solvents,[11] where ultrafast photoinduced electron transfer has been observed from solvent to an electron-accepting solute. Here, orbital overlap-dependent interactions such as those which mediate charge transfer from solvent to solute probably act between solvent molecules also, permitting some extent of cooperative charge delocalization.

The theoretical framework established in Section 2 may also assist the detailed interpretation of recent studies of transient radical diffusion in various solvents, probed by the transient grating method,[12] in which diffusion coefficients of the transient radicals are reported to be 2−3 times smaller than those of the parent molecule. These observations suggest the existence of a specific radical−molecule interaction. That work inspired a resonance Raman study of a transient neutral radical[13] in which the linewidths of the radical Raman bands were found to be much larger than those of the parent molecules, thus providing further evidence for a strong interaction between radicals and solvent. We will not, however, pursue this further in the present contribution.

The theory introduced in the present work deals explicitly with the interaction between a solute ion (radical cation) and the surrounding molecules or atoms in a small cluster. It is known that ionization potentials of aromatic (or olefinic in this case) "solute" molecules are shifted to lower energy in rare gas clusters.[14] The magnitude of this shift, typically a few hundred cm^{-1}, depends upon the number and type of rare gas "solvent" atom. This has been attributed previously to charge-induced dipole interactions; however the present work examines the problem in detail, using it as a paradigm for the suggestions

* Corresponding author. E-mail: g.scholes@ic.ac.uk.
† Imperial College of Science, Technology and Medicine.
‡ The University of Melbourne. E-mail: HARCUS@rubens.its.unimelb.edu.au.
⊗ Abstract published in *Advance ACS Abstracts,* January 1, 1997.

S1089-5639(96)02016-6 CCC: $14.00

established in the theory of Section 2. The ethene$^+$...Ar complex was chosen to study as a specific model example.

In Section 2, the solvation of a charged solute in a small cluster is examined from the perspective introduced in a recent study of electronic factors in electronic energy transfer,[15] revealing that a charge "delocalization" mechanism may be operative in certain systems. This is due primarily to charge-transfer effects, which have recently been shown to be significant in the stabilization of (neutral ground state) molecular dimers by Amovilli and McWeeny.[16] Such charge-transfer effects become significant when molecules are close enough that their charge distributions begin to interpenetrate. At larger distances, the primary interactions are polarization and dispersion interactions which can be well understood in terms of the properties of the separated molecules.[17] The key conclusion of the present work is that such intermolecular (and therefore intermolecular orbital overlap-dependent) charge-transfer resonances appear to play a significant role in delocalizing charge among a charged ("solute") molecule and suitably proximate neutral ("solvent") molecules, more so than the analogous interactions in a neutral cluster.

In this paper, we report the results of *ab initio* molecular orbital (MO), localized molecular orbital (LMO), and valence-bond (VB) studies of the $C_2H_4^+$...Ar complex. The purpose of the calculations is to characterize the structure and properties of the complex and to provide a VB rationalization for the origin of its stability. A study of the structures and ionization potentials of a series of ethene...(rare gas) complexes is reported elswhere.[18]

2. Theoretical Considerations of Charge "Solvation"

In this section the origins of charge-transfer resonance interactions in an ionized van der Waals heterocomplex are elucidated. Specifically, we investigate those interactions which depend upon the degree of intermolecular orbital overlap, shown in this work to play an important role in the stabilization of radical−solvent complexes. We do not consider dispersion, polarization, or induction interactions. Although such interactions make a significant contribution to the interaction energy, they do not specifically delocalize charge. Terms explicitly involving intermolecular orbital overlap are retained to second-order in overlap since the molecules are assumed to be weakly-interacting. Core electrons are not considered explicitly, but are included in all expressions via the effective one-electron integrals h_{ii} and h_{ij}, as discussed previously.[15]

With A = Ar and B = C_2H_4, the ground-state wavefunction for the $(AB)^+$ complex is given approximately by

$$\Psi(AB)^+ = N\{\psi_I(AB^+) + \lambda\psi_{II}(A^+B)\} \tag{1}$$

where λ is a mixing coefficient, and in which we shall assume that $\psi_I(AB^+)$ and $\psi_{II}(A^+B)$ are normalized, and that other configurations such as $\psi_{III}(A^{2+}B^-)$ and $\psi_{IV}(A^-B^{2+})$ make negligible contributions to this linear combination.

The stabilization energy for the complex, relative to the infinitely-separated dissociation products with energy E°_I is given by

$$W(AB)^+ = E_I - E^\circ_I + (2\lambda T_{I,II} + \lambda^2 T_{II,II})/(1 + 2\lambda S_{I,II} + \lambda^2) \tag{2}$$

$$\equiv E_I - E^\circ_I + \Delta E_{res} \tag{3}$$

in which $E_I \equiv H_{I,I} = \langle\psi_I|H|\psi_I\rangle$, $S_{I,II} = \langle\psi_I|\psi_{II}\rangle$, $T_{I,II} = H_{I,II} - S_{I,II}E_I$, $H_{I,II} = \langle\psi_I|H|\psi_{II}\rangle$, and $T_{II,II} = E_{II} - E_I \equiv A_{I,II}$. For a given geometry of the complex, the ΔE_{res} of eq 3 is the resonance stabilization energy that arises when $\psi_I(AB^+)$ and $\psi_{II}(A^+B)$ interact.

For a small value of the mixing coefficient λ in eq 1 such that $\lambda \approx -T_{I,II}/A_{I,II}$, the resonance stabilization energy may be expressed according to

$$\Delta E_{res} = -T_{I,II}{}^2/A_{I,II} \tag{4}$$

in which the denominator of eq 2 has been approximated to unity.

We now deduce an expression for the λ of eq 1 for the $(Ar-C_2H_4)^+$ complex using both LMO and VB formulations of the wavefunctions for the complex. The active-space electrons are assumed to be the π-electron of $C_2H_4^+$ and the argon electrons that occupy the valence shell atomic orbital (AO) that overlaps best with the π-electron orbitals of $C_2H_4^+$. The relevant AOs are designated as *a* (Ar) and as *b* and *c* ($C_2H_4^+$), with *a* and *c* located on non-neighbor argon and carbon atomic centers.

For the LMO treatment, we have constructed bonding and antibonding π-electron molecular orbitals (MOs), $\pi = N_\pi(b + c)$ and $\pi^* = N_{\pi^*}(b - c)$. We consider the eight $S = M_S = {}^1/_2$ spin LMO configurations of the following equations:

$$\psi_1 = N_1|Ra^\alpha\pi^\alpha a^\beta|, \qquad \psi_2 = N_2|Ra^\alpha\pi^{*\alpha}a^\beta| \tag{5}$$

$$\psi_3 = N_3|Ra^\alpha\pi^\alpha\pi^\beta|,\ \psi_4 = N_4(|Ra^\alpha\pi^{*\alpha}\pi^\beta| + |R\pi^\alpha\pi^{*\alpha}a^\beta|) \tag{6}$$

$$\psi_5 = N_5(|R\pi^\alpha a^\alpha\pi^{*\beta}| + |R\pi^{*\alpha}a^\alpha\pi^\beta|), \qquad \psi_6 = N_6|Ra^\alpha\pi^{*\alpha}\pi^{*\beta}| \tag{7}$$

$$\psi_7 = N_7|R\pi^\alpha\pi^{*\alpha}\pi^\beta|, \qquad \psi_8 = N_8|R\pi^\alpha\pi^{*\alpha}\pi^{*\beta}| \tag{8}$$

where $R = (1s_C)^4(\sigma_{CH})^8(\sigma_{CC})^2(Ar^{2+})$ represents the 30 core electrons. The normalized wavefunctions of the following equations (eqs 9 and 10) may hence be constructed for the ψ_I-(AB^+) and $\psi_{II}(A^+B)$ configurations of eq 1:

$$\psi_I(AB^+) = d_1\psi_1 + d_2\psi_2 \equiv N_I(\psi_1 + \lambda_2\psi_2) \tag{9}$$

$$\psi_{II}(A^+B) = d_3\psi_3 + d_4\psi_4 + d_5\psi_5 + d_6\psi_6 \equiv N_{II}(\psi_3 + \lambda_4\psi_4 + \lambda_5\psi_5 + \lambda_6\psi_6) \tag{10}$$

The wavefunction for the complex may then be expressed as

$$\Psi(AB)^+ = N\{d_1\psi_1 + d_2\psi_2 + \lambda(d_3\psi_3 + d_4\psi_4 + d_5\psi_5 + d_6\psi_6)\} \tag{11}$$

$$= \sum_{j=1}^{6} C_j\psi_j$$

$$= N\{\psi_I(AB^+) + \lambda\psi_{II}(A^+B)\} \tag{12}$$

with

$$\lambda = [\sum_{i,j=3}^{6} C_iC_jS_{ij}]^{1/2}/N \tag{13}$$

in which the C_i are variationally-determined, $S_{ij} = \langle\psi_i|\psi_j\rangle$, and $N = (C_1^2 + 2C_1C_2S_{12} + C_2^2)^{0.5}$. Equation 13 enables λ to be estimated from the C_i coefficients of the variationally-best linear combination of ψ_1 to ψ_6. The resulting expressions for the d_i coefficients for eqs 9 and 10 are given by eqs 14 and 15, respectively:

$$d_i = C_i/N \qquad i = 1, 2 \tag{14}$$

$$d_i = C_i/[\sum_{\mu,\nu=3}^{6} C_\mu C_\nu S_{\mu\nu}]^{0.5} \qquad i = 3, 4, 5, 6 \tag{15}$$

The same type of approach may be used for a VB determination of λ, with the *b* and *c* AOs replacing the π and π^* MOs in the Slater determinants. The appropriate Lewis VB structures are displayed in Figure 2, where their wavefunctions are designated as Φ_i rather than as ψ_i. However, because Φ_1 and Φ_2 are almost degenerate, we use $\psi_1 = (\Phi_1 + \Phi_2)/(1 + \langle\Phi_1|\Phi_2\rangle)$ and $\psi_2 = (\Phi_2 - \Phi_1)/(1 - \langle\Phi_1|\Phi_2\rangle)$ (i.e., the ψ_1 and ψ_2 of eq 5) instead of Φ_1 and Φ_2 in order to obtain second-order perturbation estimates of λ in the VB treatment. The ψ_3 to ψ_8 and Φ_3 to Φ_8 are the charge-transfer configurations, which only contribute to the Ψ for the (nondissociated) complex. The correspondence between the LMO and VB representations of the CT configurations is: $\psi_3 = (\Phi_3 + \Phi_5 + \Phi_6)$, $\psi_4 \approx \Phi_4$, $\psi_5 = (\Phi_3 - \Phi_5 + \Phi_6)$ and $\psi_3 = (\Phi_5 + \Phi_6 - \Phi_3)$, where normalization has been omitted, and it is noted that ψ_4 is actually more general than Φ_4 (i.e., it is a linear combination of "Φ_4-like" structures).

The results of the VB and LMO calculations reported below in Section 5 show that ψ_1 is overwhelmingly the dominant contributor to each of Ψ_I and Ψ, and therefore it is a valid approximation to set $c_2 = 0$, and to write $\lambda_i \equiv C_i/C_1 = -T_{i1}/A_{i1}$ with $T_{i1} = H_{i1} - S_{i1}E_1$, thereby obtaining approximate expressions for d_i in terms of the C_i coefficients obtained from the variational calculations.

The simplest perturbation approach to the development of an approximate expression for the ΔE_{res} of eq 4 is therefore to use the following equation:

$$\Delta E_{res} \approx -T_{13}^2/A_{13} - T_{14}^2/A_{14} - T_{15}^2/A_{15} - T_{16}^2/A_{16} \tag{16}$$

in which $T_{ij} = H_{ij} - S_{ij}E_i$ and $A_{ij} = E_j - E_i$; the configuration designated as "1" refers to the LMO configuration ψ_1, and the 3 to 6 designations refer to either the LMO configurations ψ_3 to ψ_6 of eqs 6 and 7 or the VB structure configurations Φ_3 to Φ_6 of Figure 2.

For the LMO calculations, it is found in Section 5 that the largest contributor to eq 16 is the first term. By examining its origin more closely, we find that it has the form given in the equation:

$$T_{13} \approx -B$$

$$A_{13} \approx h_{aa} - h_{bb} + (aa|aa) - (bb|bb) \tag{17}$$

$$\approx \mathrm{IP(B)} - \mathrm{IP(A)}$$

where the general notation used for integrals is that employed previously,[17c] EA(N) is the electron affinity of molecule N and IP(N) is the ionization potential of the (neutral) molecule N. *B* is the electronic transfer matrix element for an electron transfer from A to B. Equation 17 thus suggests that there should be a strong relationship between the magnitude of the ΔE_{res} of eq 16 and the difference in ionization potentials of solute and solvent.

3. Molecular Orbital Calculations

Ab initio molecular orbital calculations were carried out using the Gaussian 94 program.[19] Geometry optimizations were undertaken using a spin-restricted Hartree−Fock (HF) reference wavefunction with second-order Møller−Plesset perturbation theory correlation corrections (MP2) using the full molecular orbital space. Gradients and frequencies were determined analytically. The 6-311G Pople basis set, augmented with standard diffuse and polarization functions, was used throughout. The atoms are labeled as (Ar)...(H3)(H4)(C1)−(C2)(H5)(H6).

TABLE 1: Optimized Geometries with Corresponding Energies (*E*) and Dipole Moments (*M*) for the Ethene$^+$...Ar Complex from the MP2(FULL) Calculations[a]

	6-311++(d,p)	6-311++(df,p)	6-311++(2df,p)
r_C	1.418	1.412	1.408
r_1	1.087	1.086	1.084
r_2	1.086	1.086	1.084
r_X	3.041	2.976	2.933
a_1	120.50	120.54	120.56
a_2	120.49	120.53	120.61
a_X	97.38	97.26	94.31
d_1	−179.34	−179.23	−179.01
d_2	0.85	0.97	1.13
d_X	89.57	89.45	90.091
E, au	−605.014 9346	−605.071 1260	−605.118 0353
M, D	7.62	7.41	7.02

[a] The atoms are labeled as (Ar)...(H3)(H4)(C1)−(C2)(H5)(H6), so that $r_C = r(1-2)$ is the C−C bond length, $r_X = r(\mathrm{Ar}-1)$, $r_1 = r(1-3) \approx r(1-4)$, $r_2 = r(2-5) \approx r(2-6)$, $a_X = \angle(\mathrm{Ar}-1-2)$, $a_1 = \angle(3-1-2)$, $a_2 = d_1 = \angle(5-2-1-3)$, $d_2 = \angle(5-2-1-4)$, $d_X = \angle(\mathrm{Ar}-2-1-3)$.

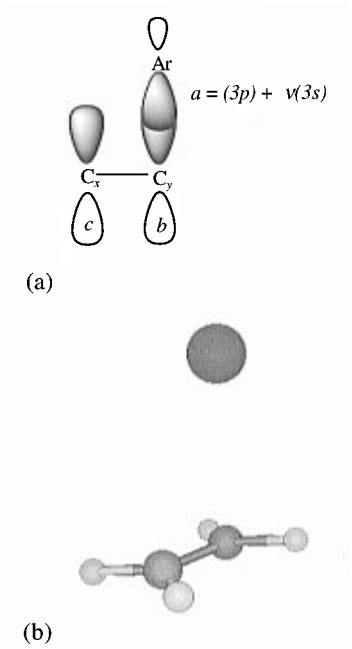

Figure 1. (a) The C_2H_4 2pπ AOs (*b* and *c*) and the odd-electron AO for Ar^+. The geometry of the complex is depicted such that the carbon and argon centers are in the plane of the page (with $r(\mathrm{Ar}-C_x) = 3.095$ Å and $\angle(\mathrm{Ar}-C_y-C_x) = 97.291°$), and the hydrogen atomic centers lie in a plane normal to the page. (b) The optimized MP2(FULL)/6-311++G(2df,p) geometry.

The complex was found to have C_1 symmetry. Optimized geometries corresponding to energy minima (i.e., no imaginary frequencies were found) determined using (d,p), (df,p), and (2df,p) polarization function sets are reported in Table 1, where the approximate C_s symmetry of the complex is used for clarity of presentation. The structure is shown in Figure 1. A most interesting point regarding this structure is that the ethene$^+$ component of the complex is almost planar, in marked contrast to the geometry determined for the isolated ethene$^+$.[20] This is most likely a result of the charge delocalization in the complex and may be considered an augmentation of the isovalent hyperconjugative and inductive effects which have been suggested to determine the torsional angle in ethene$^+$.[21]

As for ethene$^+$, most of the positive charge in ethene$^+$...Ar is found to reside on the hydrogens. For ethene$^+$ we find atomic charges to be $Q_C = 0.019$ and $Q_H = 0.240$, compared with $Q_{C1} = 0.035$, $Q_{C2} = -0.115$, $Q_{H3} \approx Q_{H4} = 0.244$, $Q_{H5} \approx Q_{H6} = 0.268$, and $Q_{Ar} = 0.057$ for ethene$^+$...Ar. If hydrogens are summed into heavy atoms, we have $Q_{C1} = 0.523$, $Q_{C2} = 0.420$, and $Q_{Ar} = 0.057$, which highlights the charge delocalization to the Ar atom predicted by the considerations of Section 2.

4. Valence Bond Structures and Orbitals

The geometry of the [ethene...Ar]$^+$ complex (cf. Figure 1) used for the VB calculations in this work was determined using the MP2/6−31++G** optimization with the ethene radical cation constrained to be planar. For the resultant equilibrium structure, the Ar atom is positioned above one of the carbon centers at a distance r(Ar−C) = 3.095 Å and angle a(Ar−C−C) = 97.291°. The aim of these calculations is to determine the origin of the stabilization, not to quantify it.

The valence-shell σ-electrons of the ethene were accommodated in C−H and C_x−C_y σ-bonding molecular orbitals (MOs) of the general form $\sigma_{CH} = (sp^2)_C + \kappa 1s_H$ and $\sigma_{CC} = (sp^2)_x + (sp^2)_y$. When structures (1) and (2) for $C_2H_4^+$ participate in resonance, the optimum value of κ for the σ_{CH} is 0.68; this value was used in all of the remaining calculations. For the VB calculations, some electron correlation was introduced into the C−C σ-bond via the inclusion of additional structures, in which the σ_{CC} bonding electrons of structures (1)−(6) have both been excited into the antibonding MO $\sigma^*_{CC} = (sp^2)_x - (sp^2)_y$ MO. The resulting VB structures obtained from this excitation are designated as (1)*, (2)*, ..., (6)*.

Allowance was made for some s−p hybridization of the argon valence-shell AOs. The *a* AO of Figure 1 was formulated as $3p + \nu 3s$, with $3s - \nu 3p$ for the corresponding orthogonal AO *a**. (The latter AO remains doubly-occupied in the calculations.) The energy optimized value for ν is ∼0.1 when structures (1)−(8) are included in the resonance scheme. When no charge transfer occurs, the configuration $(a)^2(a^*)^2$ for a free argon atom is equivalent to $(3s)^2(3p)^2$.

The in-plane Ar p orbital will overlap with some of the σ-orbitals of $C_2H_4^+$, rather than with the π-orbitals. Therefore, additional VB structures would need to be included in the calculations, which would increase the calculated charge-transfer effect. We have decided to consider only the π-electron interactions. We have not considered the polarization of the Ar in the field of $C_2H_4^+$. To investigate the resulting polarization and induction interactions (and dispersion interactions), we would need to include additional VB structures and AOs. The general procedure is outlined here.

For two molecules A and B, we introduce orbitals ϕ°_A, ϕ°_B, ϕ'_A, and ϕ'_B. Orbitals ϕ°_A and ϕ°_B are the SCF molecular orbitals which are occupied in the ground state of A and B, respectively, and ϕ'_A and ϕ'_B are "excited" orbitals of the respective fragments satisfying Brillouin's theorem. These orbitals are not virtual SCF orbitals, but are functions suitable for describing correctly the properties of the indivdual molecules which are connected with intermolecular forces. The wavefunctions Φ°_A and Φ°_B represent ground-state SCF wavefunctions for A or B and are constructed out of orbitals ϕ°_A or ϕ°_B. Functions Φ'_A and Φ'_B are perturbed states of A or B and are obtained from ground-state functions when one occupied MO, ϕ°_A, is replaced by an excited orbital, ϕ'_A; these represent "local single excitations". The following kinds of structures would be included in the VB calculations.

(i) $\{\Phi^\circ_A\Phi^\circ_B\}$. In the long-range region these describe the electrostatic interactions.

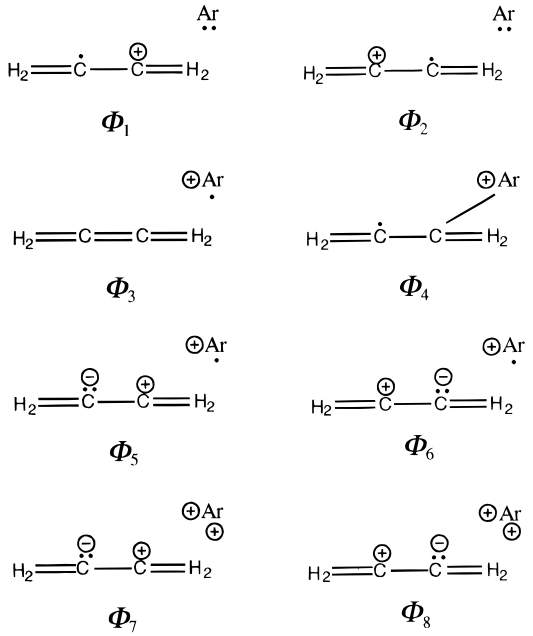

Figure 2. Canonical Lewis VB structures: $\Phi_1 = |Ra^\alpha a^\beta c^\alpha|$, $\Phi_2 = |Ra^\alpha a^\beta b^\alpha|$, $\Phi_3 = |Ra^\alpha b^\alpha c^\beta| + |Ra^\alpha c^\alpha b^\beta|$, $\Phi_4 = |Ra^\alpha b^\beta c^\alpha| + |Rb^\alpha a^\beta c^\alpha|$, $\Phi_5 = |Ra^\alpha c^\alpha c^\beta|$, $\Phi_6 = |Ra^\alpha b^\alpha b^\beta|$, $\Phi_7 = |Rb^\alpha c^\alpha c^\beta|$, $\Phi_8 = |Rb^\alpha b^\beta c^\alpha|$. $R = (1s_C)^4(\sigma_{CH})^8(\sigma_{CC})^2(Ar^{2+})$ denotes the core electrons.

(ii) $\{\Phi^\circ_A\Phi'_B\}\{\Phi'_A\Phi^\circ_B\}$. These represent A in the ground state interacting with B in the perturbed state and vice versa. In the long-range limit they express polarization effects.

(iii) $\{\Phi'_A\Phi'_B\}$. These represent perturbed molecule A interacting with perturbed molecule B, and in the long-range region describe the dispersion energy.

Such terms are expected to be around the same order of magnitude as the charge-transfer interactions considered in the present work.

Pilot calculations indicated that the $C_2H_4^+$...Ar VB structures (1) and (2) of Figure 2 would always be the dominant structures, with fairly similar contributions from each of them. Therefore, prior to any polarization of the C−H bonds, each carbon atom of $C_2H_4^+$ carries a formal charge of +0.5. For the carbon 2s and 2p AOs, we have assigned exponent values which we have obtained by adding 0.175/2 = 0.0875 (i.e., a Slater-type correction) to their "best atom" exponents. The carbon 1s and the argon 1s−3p exponents were assigned "best atom" values, and a value of 1.2 was used for the hydrogen 1s exponent. The conclusions that are obtained from this study should not depend critically on the values assigned to the exponents of the AOs.

Due to a reduction in symmetry, additional variational parameters may be introduced into the calculations for the complex, for example, to take account of a small degree of polarization of the C−C σ-bond, which will only stabilize further the complex relative to the dissociation products. It is not necessary to give consideration to these parameters here in order to demonstrate that the charge-transfer interactions are responsible for the stability of the complex relative to its dissociation products. Inclusion of these variational parameters will lead to further stabilization of the complex relative to the dissociation products.

The calculations were performed using the *ab initio* program prepared by Roso.[22] In the subsequent tables, we report energies (E, au), Coulson−Chirgwin structural weights (W_i), and the magnitudes of the coefficients (C_i) of the normalized Ψ_i and Φ_i.

TABLE 2: Coefficients Obtained from the LMO Calculations and Coefficients of the Normalized Φ_i for VB Structures[22d] (1)−(8) of Figure 2[a]

MO	C_i	C_i	C_i^a	d_i^b	d_i^c
ψ_1	0.992 95	0.992 95	1.000 00	0.999 99	
ψ_2	0.004 37	0.004 37	0.002 35	0.004 40	
ψ_3	−0.073 83	−0.073 83	−0.063 09	0.860 31	0.961 39
ψ_4	−0.044 71	−0.044 72	−0.035 05	0.521 02	0.273 27
ψ_5	−0.010 83	−0.010 83	−0.001 40	0.126 23	0.007 31
ψ_6	−0.016 63	0.016 63	−0.009 84	0.193 79	0.028 21
ψ_7	0.000 26				
ψ_8	0.000 07				
VB	C_i	C_i	C_i^a	d_i^b	d_i^c
ψ_1	0.992 95	0.992 95	1.000 00	0.999 99	
ψ_2	0.004 37	0.004 37	0.002 35	0.004 40	
Φ_3	−0.035 69	−0.035 69	−0.055 36	−0.415 82	−0.820 68
Φ_4	0.045 35	0.045 35	0.055 86	0.528 44	0.007 41
Φ_5	−0.010 93	−0.010 93	−0.007 45	−0.127 37	−0.191 39
Φ_6	−0.027 65	−0.027 64	−0.024 01	−0.322 11	−0.237 51
Φ_7	−0.000 11				
Φ_8	0.000 23				

[a] $C_i = -T_{i1}/A_{i1}$. [b] Equations 14 and 15. [c] Variational linear combination of ψ_3 to ψ_8 or Φ_3 to Φ_8 for LMO and VB treatments, respectively. For the VB calculations, $\psi_1 = N_1(\Phi_1 + \Phi_2)$, $\psi_2 = N_2(\Phi_1 - \Phi_2)$.

5. Results and Discussion

To investigate the stabilization of the ethene$^+$...Ar complex according to the model developed in Section 2, we have considered the equilibrium geometry only. Some further calculations at various ethene$^+$−Ar separations were undertaken, but are not reported here since it is quite clear from our studies of the complex that the charge-transfer effects contribute to its stabilization.

In Table 2, we report the results of the full variational LMO and VB treatments for the wavefunction of the complex which is based on the following equation:

$$\Psi = \sum_{j=1}^{8} C_j \psi_j \tag{18}$$

The results are expressed in terms of eqs 1, 9, 10, and therefore 11. They indicate that the dominant configuration contributing to the wavefunction is ψ_1 of eq 5 and that ψ_3, which involves double occupation of the C−C π-bonding MO, is the primary charge-transfer configuration (i.e., the primary contributor to the $\psi_{II}(A^+B)$ of eq 1). Omission of the ψ_7 and ψ_8 configurations, which contribute to an additional configuration which may be included in eq 1, $\psi_{III}(A^{2+}B^-)$, hardly affects the calculated energy. It may also be noted that the d_3 to d_6 coefficients of eq 11 for the ψ_3 to ψ_6 that contribute to the normalized Ψ-$(AB)^+$ differ substantially from those obtained when they are determined variationally for $\psi_{II}(A^+B)$ when $\psi_I(AB^+)$ is excluded from the calculations.

The close correspondence between our LMO and VB descriptions of $\Psi(AB)^+$ is clearly evident. The second-order perturbation estimates of the C_i (i.e., $C_i \approx -T_{i1}/A_{i1}$) are provided also in Tables 1 and 2 (for the LMO and VB treatments, respectively) and are seen to be in fair agreement with those calculated from the full variational calculations with the six configurations included. As expected, the parameter λ for eq 1 has a small value.

In Table 3 the calculated electronic transfer matrix elements T_{i1} and energy gaps A_{i1} are collected. A close correspondence between the resonance stabilization energy determined by the full variational treatment and using these matrix elements via eq 16 is evident.

TABLE 3: T_{1j} and A_{1j} Matrix Elements from VB and LMO Calculations as Well as the Resonance Stabilization Energy Determined (a) from Equation 16 and (b) Variationally

	VB	LMO
T_{12}	−0.000 608	−0.006 08
T_{13}	0.014 271	−0.016 156
T_{14}	−0.015 097	0.015 225
T_{15}	0.004 840	−0.006 751
T_{16}	0.014 143	−0.001 113
A_{12}	0.259 094	0.259 094
A_{13}	0.257 813	0.256 287
A_{14}	0.324 402	0.434 387
A_{15}	0.649 597	0.686 035
A_{16}	0.588 928	0.793 647
ΔE_{res} (a)	−0.001 86	−0.001 620
ΔE_{res} (b)	−0.001 83	−0.001 830

TABLE 4: Results of Calculations for the $C_2H_4^+$...Ar Dissociation Products (i.e., Infinitely Separated $C_2H_4^+$ and Ar)[a]

	W (i)	W (ii)
(1), (2)	0.500 (0.6381)	0.498 (0.6365)
(1)*, (2)*		0.002 50 (0.0451)
E (au)	−603.113 478	−603.123 099

[a] The same geometry for $C_2H_4^+$ has been employed here as in the complex. E is the total electronic energy in au. We have tabulated W_i, the VB normalized weight of structure i, and (in parentheses) C_i, the corresponding mixing coefficient. Obviously, we need to consider only the Lewis structures (1), (2), (1)*, and (2)* of Figure 2 since there is no interaction between fragments of the complex.

In Tables 4 and 5, we report the results of VB calculations for resonance between the following sets of the Lewis structures of Figure 2:

(a) The $C_2H_4^+$...Ar structures (1) and (2) for (i) the dissociation products and (ii) the complex. The same geometry for $C_2H_4^+$ has been assumed in both calculations. It is evident that the complex is unstable relative to the dissociation products in this case. We note that polarization of the electronic charge distributions has not been introduced into any of these calculations. This may be significant, but is not immediately relevant for the point we wish to examine.

(b) Structures (1)−(8) for the complex. The charge-transfer structures (3)−(6) naturally do not contribute to the energy of the dissociation products. The results of these calculations indicate that structures (7) and (8) make negligible contributions to the ground-state resonance scheme, and therefore they have been omitted from the calculations of (d) and (e).

(c) The structures of (a), together with structures (1)* and (2)*. It is seen that such an introduction of correlation into the C−C bond lowers the energies, but the complex remains unstable relative to the dissociation products, as in case (a).

(d) Structures (1)−(6) and (1)*−(6)*.

(e) Structures (1)−(6) and (3)*−(6)*, thereby introducing C−C σ-electron correlation into the charge-transfer structures only.

Due primarily to basis set limitations (and also to some extent, the absence of appreciable electron correlation), the VB energies are substantially higher than the those collected in Table 1. However, the VB calculations do suggest a small degree of stability for the complex relative to the Ar + $C_2H_4^+$ dissociation products. The stability is calculated to arise from the contributions of the charge-transfer structures (3)−(6) (and when appropriate (3)*−(6)*) to the resonance schemes. Exclusion of the charge-transfer structures (in other words, the ΔE_{res}) renders the complex unbound. Owing to the explicit overlap dependence of ΔE_{res}, it is expected that use of larger basis sets

TABLE 5: Results of VB Calculations of the $C_2H_4^+$...Ar Complex[a]

	W (i)	*W* (ii)	*W* (iii)	*W* (iv)	*W* (v)
(1)	0.503	0.500	0.500	0.498	0.500
(2)	0.497	0.489	0.495	0.487	0.489
(3)		0.003 44		0.003 45	0.003 89
(4)		0.004 76		0.004 71	0.005 08
(5)		0.000 43		0.000 43	0.000 48
(6)		0.002 07		0.002 06	0.002 24
(7)		1.58×10^{-7}			
(8)		9.37×10^{-7}			
(1)*			0.002 36	0.002 35	
(2)*			0.002 34	0.002 30	
(3)*				0.000 02	0.000 02
(4)*				0.000 02	0.000 03
(5)*				0.000 00	0.000 00
(6)*				0.000 01	0.000 01
E (au)	−603.111 791	−603.113 618	−603.121 413	−603.123 239	−603.113 757
E_{int} (eV)	+0.045 9	−0.003 8	+0.045 9	−0.003 8	−0.007 6

[a] Energies obtained by considering resonance between various sets of the Lewis structures of Figure 2 are compared. *E* is the electronic energy in au, W_i is the VB normalized weight of structure *i* (indicating the significance of that structure in the wavefunction), and *N* is the normalization coefficient. E_{int} is the interaction energy upon forming the complex from the dissociation products of Table 4.

(such as that used to determine the geometry of the complex) would increase the intermolecular orbital overlap significantly. With a more flexible basis set, other interactions (not considered here) such as polarization interactions will become more significant also.

Because of the large value for the second ionization potential for argon (27.6 eV), the $C_2H_4^-$...Ar^{2+} structures (7) and (8) make negligible contributions to the ground-state resonance scheme. Allowance for C−C σ-electron correlation in structures (1)−(6) hardly affects the value of the stabilization energy for the complex, cf. 0.000 14 au (ca. 24 cm^{-1}), from Table 5. Of course, when the correlation is introduced only into the charge-transfer structures, the value of the stabilization energy increases to 0.00028 au.

Further consideration of the results of Section 2 leads to the suggestion that the charge delocalization effect (via the charge-transfer interactions of structures (2)−(6) in Figure 2 or the ψ_1 and ψ_3 of eqs 5 and 6) should be more significant than the corresponding charge-transfer interaction in the neutral closed shell system. We therefore ascribe this as the primary origin of the red shifts of ionization potentials in closely-bound solute...(rare gas) clusters. A corollary is that this red shift will be quite sensitive to the ionization potential of the solvent atom (cf. eqs 16 and 17); for example, a trend should be observed for ionization potentials of the series ethene$^+$...X (X = He, Ne, Ar). This has indeed been found in our recent theoretical studies.[18]

The supermolecule approach to calculating intermolecular interactions is widely used. One problem which must be considered is basis set superposition error (BSSE). This causes an unphysical lowering of the dimer energy.[23] Unlike the supermolecule approach, it is possible to exclude the BSSE effect from some VB calculations in a clear physical manner. However, this approach is only valid for systems in which ionic structures are excluded and thus is dependent on the critical choice of resonance structures included in the VB. This is possible for the long-range interactions such as dispersion and polarization, discussed in Section 4, but obviously is not for the charge-transfer effects studied in the present work. A counterpoise correction could be made, but it is expected that BSSE will be small,[24] and will not obscure the conclusions of our study.

Further studies would be necessary to disentangle charge delocalization (attenuated strongly with separation between A and B^+) and polarization effects (capable of acting over larger separations). More elaborate VB calculations or the perturbation approaches developed for van der Waals clusters[25] could be used. It is possible that the charge-induced polarization of A could increase the significance of the charge delocalization by increasing the overlap density between the molecules.

In a recent *ab initio* study of anion solvation in water clusters,[8] an increasing shift of electron density from the halide anion to the water molecules was revealed as the number of water molecules was increased. Recent experimental studies have suggested that charge separation between a *solvent* donor and a solute acceptor occurs significantly faster than present theory can easily rationalize.[11] The present work may have implications for the origin of these phenomena.

6. Conclusions

The aim of the present work was to examine the primary interactions between a charged molecule and a neutral molecule which are close enough that their orbitals interpenetrate (as may be the case in clusters or in the condensed phase). At large separations we need to consider only the electrostatic, polarization, and dispersion interactions. The present work suggests that at close separations one should consider also the charge-transfer (CT) interactions associated with nonorthogonality effects (penetration interactions).[16,17] These CT effects appear to provide an efficacious charge delocalization mechanism along the lines proposed for the C_2H_4...Ag^+ complex,[26] where (analogously to the present $C_2H_4^+$...Ar pedagogical example) the complex is rendered stable by resonance between the VB structures $H_2C{=}CH_2$...Ag^+ and $H_2C^+{-}CH_2{-}Ag$. The work of Mulliken is also especially relevant.[21,27] The advantage of the LMO and VB treatments employed in the present work is that they allow a natural separation between polarization and CT terms. It could therefore be shown that the CT interaction provides a key contribution to the stabilization of the $C_2H_4^+$...Ar complex. We have also obtained some clues to the origin of stabilization in specific solute−solvent complexes. The development of Section 2 implies that there should be a strong relationship between the magnitude of the ΔE_{res} of eq 16 and the difference in ionization potentials of solute and solvent.

Acknowledgment. The EPSRC is gratefully acknowledged for financial support. G.D.S. thanks the Ramsay Memorial Fellowship Trust for the award of a fellowship. We are indebted to and thank Dr. W. Roso for his *ab initio* program; Dr. F. L.

Skrezenek, Mr. P. Wolynec, and Ms. J. McColl either for the installation or for the redimensioning of the program; the ITS University of Melbourne, for a special PARAGON account; and the ATP for financial support.

References and Notes

(1) (a) Reichardt, C. *Solvents and Solvent Effects in Organic Chemistry*, 2nd ed.; VCH: Weinheim, 1990. (b) Liptay, W. *Angew. Chem., Int. Ed. Engl.* **1969**, *8*, 177. (c) Mataga, N.; Kubota, T. *Molecular Interactions and Electronic Spectra*; Dekker: New York, 1970. (d) Amos, A. T.; Burrows, B. L. *Adv. Quantum Chem.* **1973**, *7*, 289.

(2) (a) Marcus, R. A.; Sutin, N. *Biochim. Biophys. Acta* **1985**, *811*, 265. (b) Hush, N. S. *Trans. Faraday Soc.* **1961**, *57*, 557.

(3) (a) Kim, H. J.; Hynes, J. T. *J. Chem. Phys.* **1990**, *93*, 5194. (b) Calef, D. F.; Wolynes, P. G. *J. Chem. Phys.* **1983**, *78*, 470.

(4) Bagchi, B.; Oxtoby, D. W.; Fleming, G. R. *Chem. Phys.* **1984**, *86*, 257.

(5) Maroncelli, M.; Fleming, G. R. *J. Chem. Phys.* **1987**, *86*, 6221.

(6) Arnold, S. T.; Eaton, J. G.; Patel-Misra, D.; Sarkas, H. W.; Bowen, K. H. In *Ion and Cluster Ion Spectroscopy and Structure*; Maier, J. P., ed.; Elsevier: Amsterdam, 1989.

(7) Jortner, J. *Z. Phys. D* **1992**, *24*, 247.

(8) Combariza, J. E.; Kestner, N. R.; Jortner, J. *J. Chem. Phys.* **1994**, *100*, 2851.

(9) de Lange, M. C. C.; Leeson, D. T.; van Kuijk, K. A. B.; Huizer, A. H.; Varma, C. A. G. O. *Chem. Phys.* **1993**, *174*, 425.

(10) (a) Gibson, E. M.; Jones, A. C.; Taylor, A. G.; Bouwman, W. G.; Phillips, D. *J. Phys. Chem.* **1988**, *92*, 5449. (b) Howell, R.; Phillips, D.; Petek, H.; Yoshihara, K. *Chem. Phys.* **1994**, *188*, 303. (c) Phillips, D.; Howell, R.; Taylor, A. G. *Proc.—Indian Acad. Sci., Chem. Sci.* **1992**, *104*, 153. (d) Kobayashi, T.; Futakami, M.; Kajimoto, O. *Chem. Phys. Lett.* **1986**, *130*, 63. (e) Shang, Q. Y.; Bernstein, E. R. *J. Chem. Phys.* **1992**, *97*, 60.

(11) Yoshihara, K.; Tominaga, K.; Nagasawa, Y. *Bull. Chem. Soc. Jpn.* **1995**, *68*, 696.

(12) Terazima, M.; Okamoto K.; Hirota, N. *J. Phys. Chem.* **1993**, *97*, 13387.

(13) Terazima, M.; Hamaguchi, H. *J. Phys. Chem.* **1995**, *99*, 7891.

(14) (a) Müller-Dethlefs, K.; Dopfer, O. *Chem. Rev.* **1994**, *94*, 1845. (b) Ben-Horin, N.; Even, U.; Jortner, J. *J. Chem. Phys.* **1992**, *97*, 5296. (c) Schmidt, M.; Mons, M.; Le Calvé, J. *Chem. Phys. Lett.* **1991**, *177*, 371. (d) Fund, K. M.; Henke, W. E.; Hays, T. R.; Selzle, H. L.; Schlag, E. W. *J. Phys. Chem.* **1991**, *85*, 3560.

(15) (a) Harcourt, R. D.; Scholes, G. D.; Ghiggino, K. P. *J. Chem. Phys.* **1994**, *101*, 10521. (b) Scholes, G. D.; Harcourt, R. D.; Ghiggino, K. P. *J. Chem. Phys.* **1995**, *103*, 9574. (c) Scholes, G. D.; Harcourt, R. D. *J. Chem. Phys.* **1996**, *104*, 5054. (d) Harcourt, R. D.; Ghiggino, K. P.; Scholes, G. D.; Speiser, S. *J. Chem. Phys.* **1996**, *105*, 1897.

(16) Amovilli, C.; McWeeny, R. *Chem. Phys.* **1995**, *198*, 71.

(17) McWeeny, R. *Methods of Molecular Quantum Mechanics*, 2nd ed.; Academic Press: New York, 1992.

(18) Scholes, G. D.; Phillips, D.; Gould, I. R. Unpublished results.

(19) Frisch, M. J.; Trucks, G. W.; Schlegel, H. B.; Gill, P. M. W.; Johnson, B. G.; Robb, M. A.; Cheeseman, J. R.; Keith, T.; Petersson, G. A.; Montgomery, J. A.; Raghavachari, K.; Al-Laham, M. A.; Zakrzewski, V. G.; Ortiz, J. V.; Foresman, J. B.; Cioslowski, J.; Stefanov, B. B.; Nanayakkara, A.; Challacombe, M.; Peng, C. Y.; Ayala, P. Y.; Chen, W.; Wong, M. W.; Andres, J. L.; Replogle, E. S.; Gomperts, R.; Martin, R. L.; Fox, D. J.; Binkley, J. S.; Defrees, D. J.; Baker, J.; Stewart, J. P.; Head-Gordon, M.; Gonzalez, C.; Pople, J. A. *Gaussian 94*, Revision B.1; Gaussian, Inc.: Pittsburgh PA, 1995.

(20) (a) Handy, N. C.; Nobes, R. H.; Werner, H.-J. *Chem. Phys. Lett.* **1984**, *110*, 459. (b) Lunell, S.; Huang, M.-B. *Chem. Phys. Lett.* **1990**, *168*, 63. (c) Scholes, G. D.; Phillips, D. P.; Gould, I. R. To be submitted.

(21) Mulliken, R. S. *Tetrahedron* **1959**, *5*, 253.

(22) (a) Harcourt, R. D.; Roso, W. *Can. J. Chem.* **1978**, *56*, 1093. (b) Skrezenek, F. L.; Harcourt, R. D. *J. Am. Chem. Soc.* **1984**, *106*, 3934. (c) Harcourt, R. D. *J. Chem. Soc., Faraday Trans.* **1991**, *87*, 1089. (d) Harcourt, R. D. *J. Organomet. Chem.* **1994**, *478*, 131.

(23) van Duijneveldt, F. B.; van Duijneveldt-van de Rijdt, J. G. C. M.; van Lenthe, J. H. *Chem. Rev.* **1994**, *94*, 1873.

(24) Harcourt, R. D. Unpublished.

(25) Jeziorski, B.; Moszynski, R.; Szalewicz, K. *Chem. Rev.* **1994**, *94*, 1887.

(26) Winstein, S.; Lucas, H. J. *J. Am. Chem. Soc.* **1938**, *60*, 836.

(27) Mulliken, R. S. *J. Am. Chem. Soc.* **1952**, *64*, 811.